Journal of Radiation Research, Vol. 58, No. 5, 2017, pp. 685–692
doi: 10.1093/jrr/rrx006
Advance Access Publication: 3 March 2017

Can clinically relevant dose errors in patient anatomy be detected by gamma passing rate or modulation complexity score in volumetric-modulated arc therapy for intracranial tumors?

Shingo Ohira[1,2], Yoshihiro Ueda[1,3], Masaru Isono[1], Akira Masaoka[1], Misaki Hashimoto[4], Masayoshi Miyazaki[1], Masaaki Takashina[2], Masahiko Koizumi[2] and Teruki Teshima[1,*]

[1]Department of Radiation Oncology, Osaka Medical Center for Cancer and Cardiovascular Diseases, Nakamichi 1-3-3, Higashinari-ku, Osaka, 537-8511, Japan
[2]Department of Medical Physics and Engineering, Osaka University Graduate School of Medicine, Suita, Japan
[3]Department of Radiation Oncology, Osaka University Graduate School of Medicine, Suita, Japan
[4]Department of Radiation Oncology, Yao Municipal Hospital, Yao, Japan
*Corresponding author. Department of Radiation Oncology, Osaka Medical Center for Cancer and Cardiovascular Diseases, Nakamichi 1-3-3, Higashinari-ku, Osaka, 537-8511, Japan. Tel: +81-6-6972-1181; Fax: +81-6-6981-1805; Email: teshima-te@mc.pref.osaka.jp
Received September 7, 2016; Revised November 28, 2016; Editorial Decision January 22, 2017

ABSTRACT

We investigated whether methods conventionally used to evaluate patient-specific QA in volumetric-modulated arc therapy (VMAT) for intracranial tumors detect clinically relevant dosimetric errors. VMAT plans with coplanar arcs were designed for 37 intracranial tumors. Dosimetric accuracy was validated by using a 3D array detector. Dose deviations between the measured and planned doses were evaluated by gamma analysis. In addition, modulation complexity score for VMAT (MCSv) for each plan was calculated. Three-dimensional dose distributions in patient anatomy were reconstructed using 3DVH software, and clinical deviations in dosimetric parameters between the 3DVH doses and planned doses were calculated. The gamma passing rate (GPR)/MCSv and the clinical dose deviation were evaluated using Pearson's correlation coefficient. Significant correlation ($P < 0.05$) between the clinical dose deviation and GPR was observed with both the 3%/3 mm and 2%/2 mm criteria in clinical target volume (D_{99}), brain (D_2), brainstem (D_2) and chiasm (D_2), albeit that the correlations were not 'strong' ($0.38 < |r| < 0.54$). The maximum dose deviations of brainstem were up to 4.9 Gy and 2.9 Gy for D_{max} and $D_{\%}$, respectively in the case of high GPR ($98.2_{\%}$ with 3%/3 mm criteria). Regarding MCSv, none of the evaluated organs showed a significant correlation with clinical dose deviation, and correlations were 'weak' or absent ($0.01 < |r| < 0.21$). The use of high GPR and MCSv values does not always detect dosimetric errors in a patient. Therefore, in-depth analysis with the DVH for patient-specific QA is considered to be preferable for guaranteeing safe dose delivery.

KEYWORDS: gamma passing rate, modulation complexity score, VMAT, QA, intracranial tumors

INTRODUCTION

Volumetric-modulated arc therapy (VMAT) has been introduced in clinical radiation oncology to improve tumor control by delivering a high dose to the tumor and/or to reduce the risk of normal tissue injury [1]. Moreover, VMAT also provides more rapid dose delivery and requires fewer monitor units (MUs) than conventional intensity-modulated radiation therapy (IMRT) [2, 3]. Thanks to these characteristics, a number of institutions have now rapidly introduced VMAT into clinical practice. Patients with intracranial tumors are expected to particularly benefit from VMAT because

these tumors are surrounded by many critical organs at risk (OARs), including the brainstem, chiasm, optic nerves and retinae. These patients are often treated using strongly modulated radiation fields with continuous variations in complex multileaf collimator (MLC) patterns, gantry speed and dose rate during delivery [4, 5], which in turn indicates the necessity for patient-specific quality assurance (QA) for VMAT to eliminate concerns about unknown factors and to guarantee safe dose delivery.

The 3D dose distribution actually delivered in a patient's body can now be reconstructed using commercially available software such as 3DVH (SUN NUCLEAR corporation, Melbourne, FL) on the basis of the measured dose distribution inside a QA phantom [6]. This measurement-guided dose reconstruction allows dose distributions calculated by a treatment planning system (TPS) to be validated, and also allows in-depth analysis with the dose–volume histogram (DVH), which provides quantitative information with regard to how much dose is absorbed for volume, and also summarizes the entire dose distribution into a single curve for each anatomic structure of interest [7].

However, patient-specific QA is commonly implemented using radiographic films, 2D or 3D array detectors [8–10] in a homogeneous phantom rather than a phantom with patient anatomy. The dosimetric deviation between the planned and the measured dose is generally evaluated with a 3% criterion for percentage difference analysis and a 3 mm criterion for distance to agreement (DTA) analysis (3%/3 mm criteria) [11]. Basran *et al.* stated that the gamma passing rate (GPR) with a 3%/3 mm criteria should be ≥95% for non–head and neck cases, and ≥ 88% for head and neck cases, which use strongly modulated radiation fields for the same reason as in intracranial tumor cases [12]. Thus, this pattern appears to imply a trade-off between treatment plan complexity and dosimetric accuracy. Masi *et al.* proposed a modulation complexity score applied to VMAT (MCSv) to predict the accuracy of the dose delivery in patient-specific QA for complex VMAT plans. They found that MCSv had a significant correlation with GPR, resulting in the lower value of MCSv being induced to larger dosimetric errors [13]. However, it is difficult to judge whether the lower values of the GPR or MCSv indicate clinically relevant dosimetric errors in patient anatomy, and few studies have investigated this question. Particularly for patients with intracranial tumors, the location and the degree of the dosimetric error may have priority over the GPR or the value of MCSv because multiple critical OARs are located near the primary tumor.

The aim of this study was to investigate whether methods conventionally used to evaluate patient-specific QA of VMAT for intracranial tumors have correlation with clinical dosimetric errors in patient anatomy.

MATERIALS AND METHODS

Patients and treatment planning

This study, which was approved by the ethics committee, included a total of 37 clinical VMAT plans for intracranial tumors: 17 for glioblastoma, 5 for astrocytoma, 9 for metastasis and 6 for others. Written informed consent was obtained from each patient. The treatment plans were designed to stipulate 24–60 Gy to cover 95% of the planning target volumes (mean ± standard deviation, 180.4 ± 137.8 cm^3) in 1–25 fractions, with 2–7 coplanar arcs by means of the TPS (Eclipse, version 11.0, Varian Medical Systems) using a Clinac 23EX linear accelerator (Varian Medical Systems, Palo Alto, CA) equipped with a Millennium 120-leaf MLC. A photon beam of 6 MV with a dose rate of 600 MUs/min was used. Dose calculations were performed using the analytic anisotropic algorithm on a 2.5-mm dose grid size. Dose constraints for OARs in conventionally fractionated plans were—maximum dose for the brainstem: 54 Gy; maximum dose for the chiasm, optic nerves, and retinae: 50 Gy. Constraints in a single fraction were—maximum dose for the brainstem: 15 Gy; maximum dose for the chiasm, optic nerves, and retinae: 10 Gy.

Gamma analysis

For patient-specific QA, doses were delivered to a helical diode array dosimeter (ArcCHECK, SUN NUCLEAR corporation) with a tough water insert. The ArcCHECK has an outer diameter of 26.6 cm and contains 1386 point detectors positioned 1 cm apart along both the cylindrical length and circumference [14]. The ArcCHECK was carefully placed at the isocenter on the top of the treatment couch by a well-trained medical physicist using a well-coordinated laser pointer system on the wall to minimize the positioning error of ArcCHECK. Before each measurement, linac output variation in a 10 × 10 cm^2 field was checked to be <1%. To quantitatively compare absolute dose distributions between the measured dose and the corresponding dose calculated from the TPS, the treatment plans were copied into the static phantom image while keeping all planning parameters consistent (beam arrangement, leaf positions, MUs, etc.), and doses were re-calculated. Gamma analysis was then performed with the evaluation criteria of 3%/3 mm and 2%/2 mm with a low-dose threshold of 10%. GPR was defined as the percentage of points satisfying the condition that the gamma index was <1. The gamma analysis in the 3DVH software consists of a three-step procedure [15]. When the first step (looking at the dose difference at the same point) does not get a given detector point passed, the software goes through the second step (looking at the DTA value). When both steps fail to pass the given detector point, the software tries to use a combination of dose difference and DTA, and to find a gamma value <1 so that the point can pass. In cases in which the GPR with 3%/3 mm was <90%, the treatment plan was re-designed, and patient-specific verification was performed again.

Calculation of modulation complexity score for VMAT plans

The concept of assessing the modulation complexity of IMRT plans was proposed by McNiven *et al.* [16], who calculated modulation complexity score (MCS) from the leaf sequence variability (LSV) parameter and the aperture area variability (AAV). The MCS was then modified for VMAT by Masi *et al.* to take account of the control points (CPs) of the arc instead of the segments [13]. The MCSv for each plan was calculated with our in-house software (MATLAB R2016a; MathWorks, Natick, MA, USA) and the overall MCSv was defined as the mean of MCSv for each arc. The MCSv was calculated from the LSV parameter, the AAV and normalized MU value (details are shown in ref. 13) [13]. The LSV was defined

for each CP considering in each bank the differences in position between adjacent MLC leaves.

$$pos_{\max}(CP) = (\max(pos_{n\in N}) - \min(pos_{n\in N}))_{leafbank} \quad (1)$$

$$LSV_{cp} = \left[\frac{\sum_{n=1}^{N-1}(pos_{\max} - |pos_n - pos_{n+1}|)}{(N-1)\times pos_{\max}}\right]_{leftbank} \times \left[\frac{\sum_{n=1}^{N-1}(pos_{\max} - |pos_n - pos_{n+1}|)}{(N-1)\times pos_{\max}}\right]_{rightbank}, \quad (2)$$

where N and pos are the number of moving leaves inside the jaws and the coordinate of leaf position, respectively. The AAV is calculated as the area defined by apertures of opposing leaves in the single CP normalized to the maximum area in the arc, defined by the maximum apertures for each leaf pair over all CPs in the arc:

$$AAA_{cp} = \frac{\sum_{a=1}^{A}((pos_a)_{leftbank} - (pos_a)_{rightbank})}{\sum_{a=1}^{A}((\max(pos_a))_{leftbank\in arc} - (\max(pos_a))_{rightbank\in arc})} \quad (3)$$

where A is the number of leaves in the arc. Finally, the MCSv is calculated using the following formula:

$$MCSv = \sum_{i=1}^{i-1}\left[\frac{(AAV_{cp_i} + AAV_{cp_{i+1}})}{2} \times \frac{(LSV_{cp_i} + LSV_{cp_{i+1}})}{2} \times \frac{MU_{cp_{i,\,i+1}}}{MU_{arc}}\right], \quad (4)$$

where $MU_{CPi,i+1}$ indicates the MU delivered between two successive CPs (i.e. CP_i and $CP_{(i+1)}$). The value of the MCSv decreases as the modulation complexity increases. Thus, MCSv = 1 indicates that the plan is designed with a fixed rectangular aperture with no leaves moving during the arc.

3D dose reconstruction in patient anatomy

DICOM RT plan, DICOM RT structure set, DICOM RT dose, patient CT dataset and measured dose data by means of the ArcCHECK were loaded into the 3DVH software. The software provided a 3D dose distribution in patient anatomy that reflected dosimetric errors during dose delivery [6]. Consequently, dose deviations in a target and OARs can be assessed using the DVH. Absolute deviations in dosimetric parameters between the 3DVH and TPS for the clinical target volume (CTV) and to the surrounding OARs (brain, brainstem, chiasm, ipsilateral optic nerve and ipsilateral retina) were calculated using the following formula:

$$Dose\ deviation\ (\%) = \left|\frac{3DVH\ dose\ (Gy) - TPS\ dose\ (Gy)}{TPS\ dose\ (Gy)}\right| \times 100\%. \quad (5)$$

Pearson's correlation coefficient was performed for the statistical measure of the strength of a linear relationship between the dose deviations and the GPR/MCSv, and the degree of association was measured by a correlation coefficient, denoted by r. The absolute value of r was defined as very weak (0–0.19), weak (0.2–0.39), moderate (0.40–0.59), strong (0.6–0.79) and very strong (0.8–1). The significance of correlations was analyzed by the two-tailed t test and a P value < 0.05 was considered to indicate statistical significance. All analyses were conducted with SPSS version 16 (SPSS Inc; Chicago, IL, USA).

RESULTS

Gamma passing rate and Modulation Complexity Score for VMAT

Table 1 shows the GPR derived from doses computed on the TPS and measured doses by means of ArcCHECK, and the MCSv calculated from the DICOM RT plan for a total of 37 VMAT plans. The GPR for all plans was above 90% with the 3%/3 mm criteria, at which an action-level was set in our patient-specific verification protocol. The percentage of plans with >95% GPR was 70.2% with 3%/3 mm criteria, but decreased to 48.6% with the more strict criteria of 2%/2 mm. The value of MCSv varied widely from 0.16 at minimum to 0.42 at maximum. The MCSv values were >0.25 and >0.35 in 89.2% and 40.5% of the plans, respectively. Correlations between GPR and MCSv are shown in Fig. 1. All treatment plans with the value of MCSv ≥ 0.3 showed ≥95% GPR with 3%/3 mm criteria (Fig. 1a), and all plans except one with the value of MCSv ≥ 0.3 showed ≥90% GPR with 2%/2 mm criteria (Fig. 1b). This indicates that the treatment beams using complexity metric are not dosimetrically robust (i.e. MCSv can predict the dosimetric results).

Dose deviation in patient anatomy

Correlations between the clinical dose deviation in patient anatomy for each evaluated organ and the GPR as well as MCSv are shown in Figs 2 and 3, respectively, and the corresponding Pearson's r values are summarized in Table 2. The two-tailed t test showed statistically significant negative correlations between clinical dose deviations and GPR for the CTV, brain, brainstem, chiasm and ipsilateral optic nerve, indicating that lower GPR resulted in larger dosimetric errors in a patient anatomy, but there were only 'weak' to 'moderate' correlations ($0.23 < |r| < 0.54$). As described in Fig. 2, clinical dose deviations varied widely from patient to patient, and the

Table 1. Statistical values of gamma passing rate (GPR) with 3%/3 mm and 2%/2 mm criteria, and modulation complexity score for VMAT (MCSv) for a total of 37 treatment plans

	GPR (3%/3 mm)	GPR (2%/2 mm)		MCSv
Mean	97.9%	92.8%		0.32
Standard deviations	2.8%	5.2%		0.07
Maximum	100%	98.9%		0.42
Minimum	90.1%	77.4%		0.16
Number of plans				
GPR > 95%	70.2%	48.6%	MCSv > 0.35	40.5%
GPR > 90%	100%	75.7%	MCSv > 0.25	89.2%

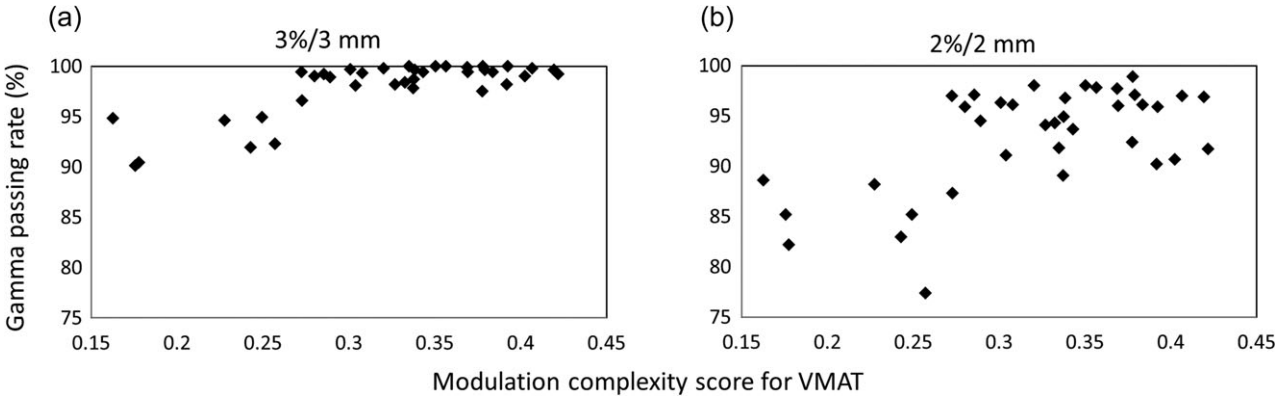

Fig. 1. Correlations between modulation complexity score for VMAT and gamma passing rate with criteria of (a) 3%/3 mm and (b) 2%/2 mm.

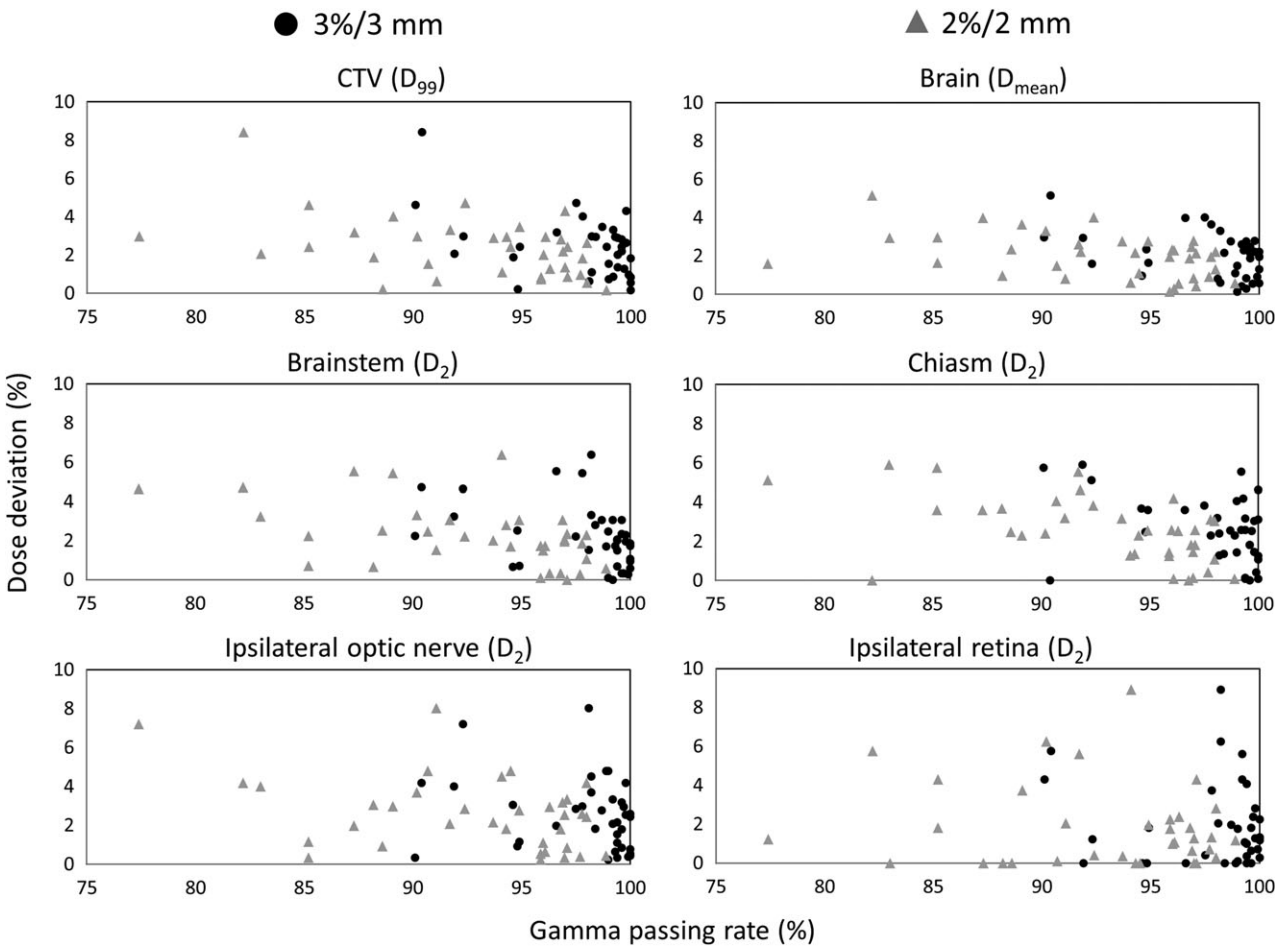

Fig. 2. Correlations between clinical dose deviation in patient anatomy and gamma passing rate with criteria of 3%/3 mm (black circle) and 2%/2 mm (gray triangle). CTV = clinical target volume, D_{99} = dose to 99% of the volume, D_{mean} = mean dose, D_2 = dose to 2% of the volume.

maximum dose deviations for brainstem (6.4%), ipsilateral optic nerve (8.0%) and ipsilateral retina (8.9%) were observed in high GPR (>95%) cases with 3%/3 mm criteria. Regarding the correlations between clinical dose deviation and the MCSv, correlations were 'very weak' to 'weak' for all evaluated organs, and no significant correlation was observed ($P > 0.05$). The maximum dose

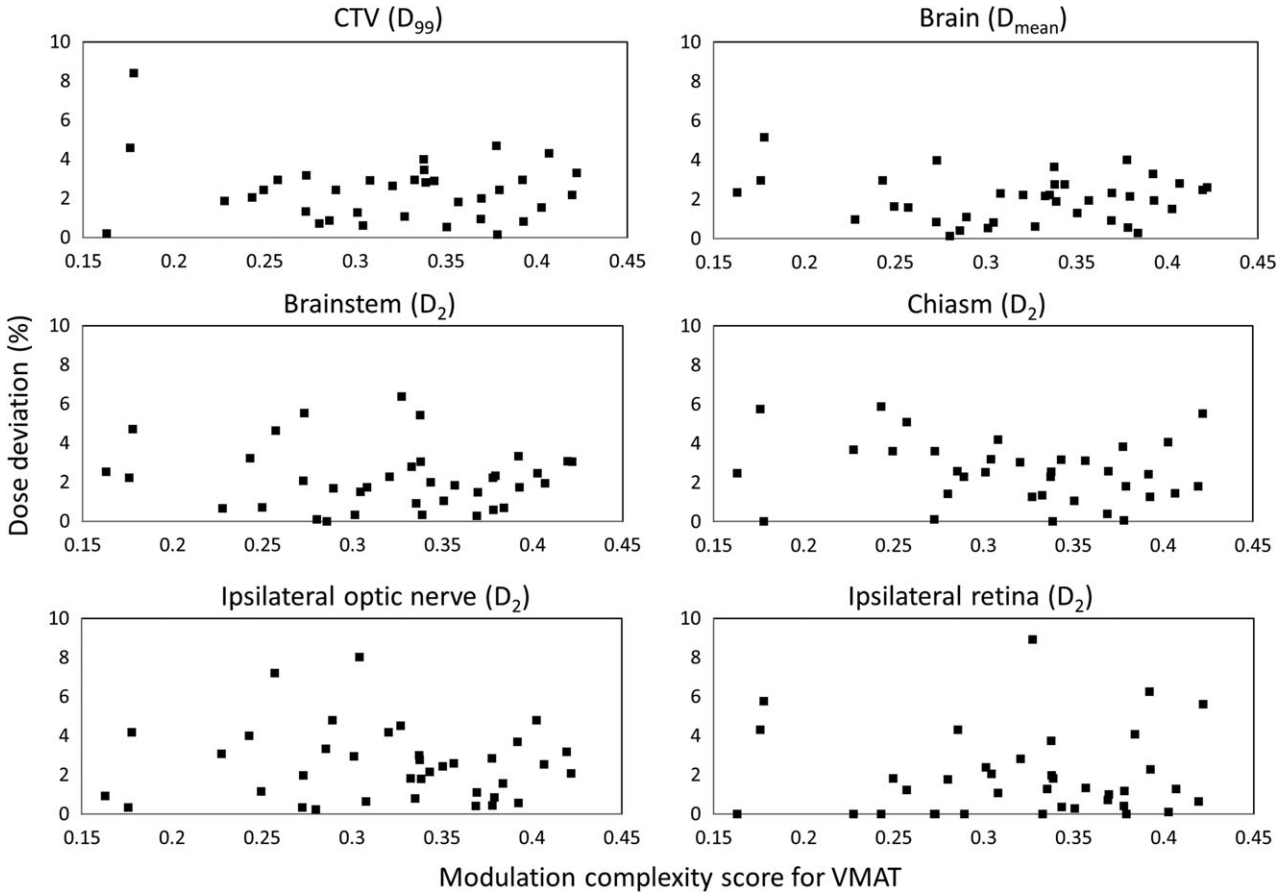

Fig. 3. Correlations between clinical dose deviation in patient anatomy and modulation complexity score for VMAT. CTV = clinical target volume, D_{99} = dose to 99% of the volume, D_{mean} = mean dose, D_2 = dose to 2% of the volume.

Table 2. Pearson correlation values (r) and two-tailed P-values for each evaluated organ

	GPR (3%/3 mm)		GPR (2%/2 mm)		MCSv	
	r	*P*	*r*	*P*	*r*	*P*
CTV (D_{99})	−0.49	0.002	−0.44	0.006	−0.19	0.24
Brain (D_{mean})	−0.41	0.013	−0.43	0.007	−0.09	0.59
Brainstem (D_2)	−0.38	0.02	−0.49	0.002	−0.11	0.54
Chiasm (D_2)	−0.41	0.013	−0.54	0.001	−0.21	0.20
Ipsilateral optic nerve (D_2)	−0.23	0.16	−0.39	0.018	−0.07	0.70
Ipsilateral retina (D_2)	−0.13	0.44	−0.11	0.51	0.01	0.95

GPR = gamma passing rate, MCSv = modulation complexity score applied to VMAT, CTV = clinical target volume, D_{99} = dose to 99% of the volume, D_{mean} = mean dose, D_2 = dose to 2% of the volume.

deviations for brainstem, ipsilateral optic nerve and ipsilateral retina were observed in the MCSv > 0.3 (Fig. 3).

Figure 4 illustrates the (a) gamma distribution with 3%/3 mm criteria, (b) dose distributions on the TPS/3DVH and 3D-GPR with 1%/1 mm criteria, and (c) DVHs of the TPS/3DVH for one of the 37 plans (Plan 9) investigated. In this case, the respective values of GPR with 3%/3 mm, GPR with 2%/2 mm criteria and MCSv were 98.2% (Fig. 4a), 94.1% and 0.33, which values were higher than the mean values of 37 plans shown in Table 1, but the dose deviations (gamma index >1 with 1%/1 mm criteria) were observed

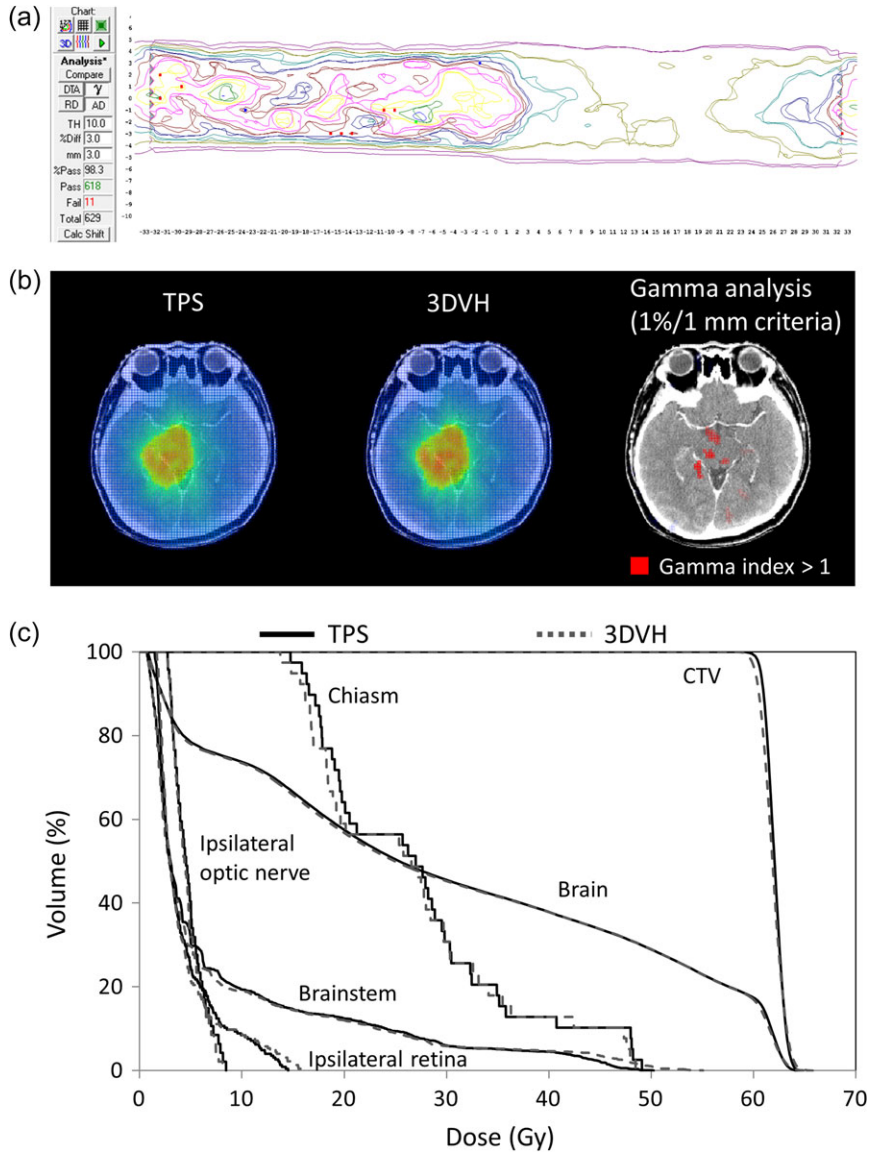

Fig. 4. Gamma distribution with 3%/3mm criteria (a) and dose distributions on the treatment planning system (TPS) and 3DVH and 3D-GPR with 1%/1 mm criteria (b), and dose–volume histograms of the TPS (solid lines) and the 3DVH (dashed lines) for Plan 9.

in the region of the brainstem (Fig. 4b). The dose deviation of the maximum dose and D_2 (which was the dose to 2% of the volume) for brainstem were up to 4.9 Gy (TPS: 50.2 Gy; 3DVH: 55.1 Gy) and 2.9 Gy (TPS: 45.1 Gy; 3DVH: 48.0 Gy), respectively (Fig. 4c). This result implies that clinically relevant dose deviations that may induce unwanted normal tissue toxicities can happen even if conventional patient-specific QA results shows high GPR or MCSv.

DISCUSSION

In this study, we investigated correlations between the methods used for evaluating conventional patient-specific QA for VMAT and clinical dose deviations in patients with intracranial tumors. It should be mentioned that the evaluation with GPR was strongly dependent on the configuration of gamma analysis. In patient-specific QA, the 3%/3 mm criteria is most commonly used, but 15% and 4% of institutions used criteria with a 5% dose difference and 5 mm distance to agreement, respectively [11]. The looser constraint would result in better GPR than more severe criteria such as 2%/2 mm or 1%/1 mm. The value of GPR is also dependent on the specified low-dose threshold, which has an impact when local gamma analysis is performed [17]. Moreover, Nelms *et al.* reported that gamma analysis for IMRT or VMAT patient-specific QA could not detect dosimetric errors such as those caused by the tongue-and-groove effect, underestimation of dose for small MLC segments, incorrect QA phantom density setting in TPS, and others [18].

3DVH software can be a solution to these problems. In the report on the accuracy of dose estimation with 3DVH, Olch *et al.* compared the composite dose to an ionization chamber and film in a solid water phantom and predicted by the 3DVH. They concluded that the dose differences with an ionization chamber were negligible and found no statistically significant differences when the doses of 3DVH and film-measured doses were compared [19]. In our present study, we reconstructed 3D doses for patients with intracranial tumors in which the tumors were surrounded by homogeneous normal brain tissues. The reconstructed dose distributions, therefore, appear to accurately represent the actually delivered dose. Although our results showed a significant correlation between clinical dose deviation for several organs and the GPR, the correlations were not strong. In contrast, no correlation was observed for the retina or optic nerve. Nelms *et al.* investigated the correlations between clinical dose deviations (CTV, parotid, spinal cord and larynx) for head-and-neck IMRT and GPR, but found a lack of correlations [10], and thus concluded that the conventional QA method was invalid because meeting its criteria did not ensure that dose errors would be clinically acceptable. Accordingly, our present results and Nelms *et al.*'s previous results did not show sufficient data to demonstrate that GPR is able to detect clinically relevant dosimetric errors in conventional patient-specific QA.

MCSv numerically measures how VMAT treatment planning uses complex MLC patterns. Masi *et al.* reported MCSv values for 142 treatment plans generated by using the Oncentra (Elekta AB, Elekta, Stockholm, Sweden) TPS (consisting of 80 plans for prostate cancers, 14 for pelvic lymph nodes, 18 for spinal tumors, 10 for mediastinal lesions and 20 for others), which ranged from 0.19 to 0.65, with a mean of 0.41 [13]. In our study, the Eclipse TPS was used and the maximum MCSv value was 0.42. The values of the MCSv varied depending on the TPSs due to different algorithms for optimization and leaf sequencing. Mcgarry *et al.* performed a virtual phantom VMAT planning exercise in a multi-institutional audit and concluded that more complex plans were created by TPSs such as Oncentra and Pinnacle (Philips Radiation Oncology Systems, Fitchburg, WI), which were independent of vendor for VMAT delivery [20]. This finding indicates that treatment plans for intracranial tumors seem to require relatively complex MLC patterns to avoid irradiating high doses to critical organs. Masi *et al.* reported that MCSv was significantly correlated with VMAT dosimetric accuracy expressed as GPR. In our study, MCSv also showed a strong and significant correlation with the GPR (Fig. 1a). This finding indicated that MCSv can detect dosimetric errors, on the basis that dose delivery with the use of small fields induces dosimetric errors due to the effect of incomplete lateral electron equilibration [21, 22]. The finite spacing resolution of diode detectors may also cause dosimetric error in small-field measurement. Although Masi *et al.* concluded that MCSv would help improve the general workflow in patient-specific QA [13], our present results showed that correlation between MCSv and clinical dose deviation was not significant for any of the organs evaluated. In turn, this indicates that relatively simple treatment plans expressed by MCSv do not ensure clinically acceptable dose errors in patient anatomy for VMAT. We therefore consider that patient-specific QA in clinical workflow cannot be simplified without careful consideration and rigorous QA, with DVH analysis for critical organs, and that this workflow may be essential in modern radiotherapy.

Three-dimensional dose distributions in patient anatomy can be now be estimated based on measured dose, using several commercially available software applications, including the COMPASS system (IBA Dosimetry, Germany), Mobius3D software (Mobius Medical Systems, Houston, TX) and Dosimetry Check software (Math Resolutions, LLC, Columbia, MD). Previous investigators have used these systems to confirm the claimed accuracy of 3D dose estimation for clinical use [23–25], and these approaches are now thought to be taking the place of conventional patient-specific QA. More recently, the interplay and motion effects of tumors such as lung cancer were quantified by means of the 4D Respiratory MotionSim module of 3DVH [26]. These effects may induce an underdose or overdose in relation to the target volume. Regarding the intracranial tumors, Hoogeman *et al.* reported that intra-organ motion generally seemed to be small if compared with other error sources (e.g. interfraction set-up errors, delineation errors, geometrical errors from internal organ motion), but that motion would significantly contribute to the margin for high-precision radiation treatments with treatment times of 15 min or longer [27]. Further study is expected to assess the intrafractional motion effects on target coverage for VMAT for intracranial tumors.

Several limitations of this study warrant mention. First, ArcCHECK diode detectors require irradiation by perpendicular treatment beams. However, non-coplanar treatment provides dosimetric advantages over coplanar treatment [28, 29]. Second, extended fields [30] might not be covered by ArcCHECK detectors because the maximum length of measurement range along the superior–inferior direction is 26 cm. Third, dosimetric parameters were evaluated in 2.5 mm grid size, but this size may be large for thin and elongate organs such as chiasm, optic nerves and retina. Fourth, the diode detectors in the ArcCHECK may be more sensitive to low-energy photon scatter than the ionization chambers. In this study, the diode detectors were calibrated with the $10 \times 10\ cm^2$ field size, and the small segments in the VMAT field might be underestimated. Olch *et al.* reported that this underestimation of the diode detectors was ~1% [19]. Finally, this study was limited to intracranial tumors only. Evaluating whether methods conventionally used to evaluate patient-specific QA can detect clinically relevant dosimetric errors for various tumor sites awaits further investigation.

In conclusion, neither high GPR nor MCSv values in patient-specific QA for VMAT showed a strong correlation with dose deviations in patients with intracranial tumors. We therefore consider that in-depth analysis with the DVH for patient-specific QA for VMAT is preferable for guaranteeing safe dose delivery.

CONFLICT OF INTEREST

The authors declare that there are no conflicts of interest.

FUNDING

This work was supported by the Japan Society for the Promotion of Science (JSPS; No. 84409) core-to-core program (No. 23003), the National Cancer Center Research and Development Fund

(No. 84409) (26-A-28), JSPS KAKENHI (No. 84409) Grant No. 15H04913, Health and Labour Sciences Research (No. 84409) Grants (H26-Cancer Policy-General-014) and the Osaka Cancer Society (No. 84409).

REFERENCES

1. Verbakel W, Cuijpers JP, Hoffmans D, et al. Volumetric intensity-modulated arc therapy vs. conventional IMRT in head-and-neck cancer: a comparative planning and dosimetric. *Int J Radiat Oncol Biol Phys* 2009;74:252–9.
2. Matuszak MM, Yan D, Grills I, et al. Clinical applications of volumetric modulated arc therapy. *Int J Radiat Oncol Biol Phys* 2010;77:608–16.
3. Palma D, Vollans E, James K, et al. Volumetric modulated arc therapy for delivery of prostate radiotherapy: comparison with intensity-modulated radiotherapy and three-dimensional conformal radiotherapy. *Int J Radiat Oncol Biol Phys* 2008;72:996–1001.
4. Quan EM, Li X, Li Y, et al. A comprehensive comparison of IMRT and VMAT plan quality for prostate cancer treatment. *Int J Radiat Oncol Biol Phys* 2012;83:1169–78.
5. Wu C, Hosier KE, Beck KE, et al. On using 3D γ-analysis for IMRT and VMAT pretreatment plan QA. *Med Phys* 2012;39:3051–9.
6. Nelms BE, Opp D, Robinson J, et al. VMAT QA: measurement-guided 4D dose reconstruction on a patient. *Med Phys* 2012;39:4228–38.
7. Khan FM. *The Physics of Radiation Therapy*, 4th edn. Philadelphia: Lippincott Williams & Wilkins (Wolters Kluwer), 2010.
8. Korevaar EW, Wauben DJ, van der Hulst PC, et al. Clinical introduction of a linac head-mounted 2D detector array based quality assurance system in head and neck IMRT. *Radiother Oncol* 2011;100:446–52.
9. Ghandour S, Matzinger O, Pachouda M. Volumetric-modulated arc therapy planning using multicriteria optimization for localized prostate cancer. *J Appl Clin Med Phys* 2015;16:5410.
10. Nelms BE, Zhen H, Tomé WA. Per-beam, planar IMRT QA passing rates do not predict clinically relevant patient dose errors. *Med Phys* 2011;38:1037–44.
11. Nelms BE, Simon JA. A survey on planar IMRT QA analysis. *J Appl Clin Med Phys* 2007;8:2448.
12. Basran PS, Woo MK. An analysis of tolerance levels in IMRT quality assurance procedures. *Med Phys* 2008;35:2300–7.
13. Masi L, Doro R, Favuzza V, et al. Impact of plan parameters on the dosimetric accuracy of volumetric modulated arc therapy. *Med Phys* 2013;40:071718.
14. Li G, Zhang Y, Jiang X, et al. Evaluation of the ArcCHECK QA system for IMRT and VMAT verification. *Phys Med* 2013;29:295–303.
15. SUN NUCLEAR corporation. *ArcCHECK® & 3DVH®—The Ultimate 4D Patient QA Solution*. sunnuclear.com (Document 1220011, Rev H, 28 September 2012, date last accessed).
16. McNiven AL, Sharpe MB, Purdie TG. A new metric for assessing IMRT modulation complexity and plan deliverability. *Med Phys* 2010;37:505–15.
17. Song JH, Kim MJ, Park SH, et al. Gamma analysis dependence on specified low-dose thresholds for VMAT QA. *J Appl Clin Med Phys* 2015;16:5696.
18. Nelms BE, Chan MF, Jarry G, et al. Evaluating IMRT and VMAT dose accuracy: practical examples of failure to detect systematic errors when applying a commonly used metric and action levels. *Med Phys* 2013;40:111722.
19. Olch AJ. Evaluation of the accuracy of 3DVH software estimates of dose to virtual ion chamber and film in composite IMRT QA. *Med Phys* 2012;39:81–6.
20. Macgarry CK, Agnew CE, Hussein M, et al. The role of complexity metrics in a multi-institutional dosimetry audit of VMAT. *Br J Radiol* 2016;89:20150445.
21. Rustgi SN, Frye DM. Dosimetric characterization of radiosurgical beams with a diamond detector. *Med Phys* 1995;22:2117–21.
22. Westermark M, Arndt J, Nilsson B, et al. Comparative dosimetry in narrow high-energy photon beams. *Phys Med Biol* 2000;45:685–702.
23. Kathirvel M, Subramanian S, Clivio A, et al. Critical appraisal of the accuracy of Acuros-XB and Anisotropic Analytical Algorithm compared to measurement and calculations with the compass system in the delivery of RapidArc clinical plans. *Radiat Oncol* 2013;8(140):1–9.
24. Clemente-Gutiérrez F, Pérez-Vara C. Dosimetric validation and clinical implementation of two 3D dose verification systems for quality assurance in volumetric-modulated arc therapy techniques. *J Appl Clin Med Phys* 2015;16:5190.
25. Liang Y, Kim GY, Pawlicki T, et al. Feasibility study on dosimetry verification of volumetric-modulated arc therapy-based total marrow irradiation. *J Appl Clin Med Phys* 2013;14:3852.
26. Tyler MK. Quantification of interplay and gradient effects for lung stereotactic ablative radiotherapy (SABR) treatments. *J Appl Clin Med Phys* 2016;17:5781.
27. Hoogeman MS, Nuyttens JJ, Levendag PC, et al. Time dependence of intrafraction patient motion assessed by repeat stereoscopic imaging. *Int J Radiat Oncol Biol Phys* 2008;70:609–18.
28. Zhong-Hua N, Jing-Ting J, Xiao-Dong L, et al. Coplanar VMAT vs. noncoplanar VMAT in the treatment of sinonasal cancer. *Strahlenther Onkol* 2015;191:34–42.
29. Liu H, Andrews D, Evans J, et al. Plan quality and treatment efficiency for radiosurgery to multiple brain metastases: non-coplanar RapidArc vs. Gamma Knife. *Front Oncol* 2016;6:26.
30. Beriwal S, Gan G, Heron D, et al. Early clinical outcome with concurrent chemotherapy and extended-field, intensity-modulated radiotherapy for cervical cancer. *Int J Radiat Oncol Biol Phys* 2007;68:166–71.